ACS Catalysis

RESEARCH ARTICLE

pubs.acs.org/acscatalysis

Bioelectrocatalytic Oxidation of Glucose in CNT Impregnated Hydrogels: Advantages of Synthetic Enzymatic Metabolon Formation

Michael J. Moehlenbrock,[†] Matthew T. Meredith,[†,‡] and Shelley D. Minteer*[,†,‡]

[†]Department of Chemistry, Saint Louis University, 3501 Laclede Avenue, St. Louis, Missouri 63103, United States

[‡]Departments of Chemistry and Materials Science and Engineering, University of Utah, 315 S 1400 E, Salt Lake City, Utah 84112, United States

Supporting Information

ABSTRACT: Enzymatic biofuel cells and bioelectrochemical sensors are often limited in performance because of their inability to utilize all of the energy confined in chemical bonds of complex molecules. Multi-enzyme cascade catalysis provides a means to remedy this limitation, but efficiencies of such electrodes can be further enhanced by improving interenzyme substrate mass transport. This consideration is demonstrated to be advantageous in biological systems, as displayed by nearly ubiquitous organization of sequential enzymes in natural metabolic pathways. This sequential organization, termed a metabolon, is examined in this work for a two-enzyme pentose phosphate pathway bioelectrode for the oxidation of glucose. This two-enzyme electrode is compared with a single enzyme, glucose dehydrogenase, and demonstrates increased performance. In addition, increases in efficiency are demonstrated through the creation of a synthetic two-enzyme metabolon versus randomly suspended enzymes immobilized within a hydrogel matrix.

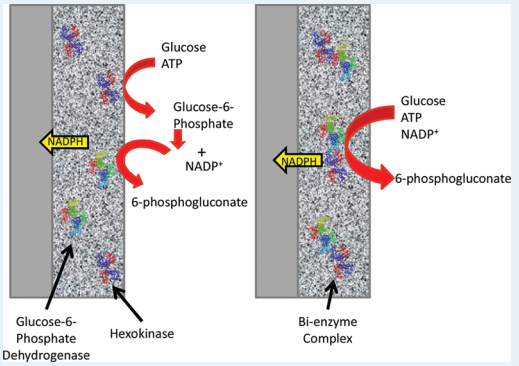

KEYWORDS: glucose biosensor, substrate channeling, biofuel cell, metabolon, pentose phosphate pathway

INTRODUCTION

In recent years, there has been tremendous growth in the development of immobilized enzyme bioelectrocatalysis for both biosensor and biofuel cell technology. Historically, the field has been isolated to the examination of single-enzyme-catalyzed, partial oxidation of key fuels, such as simple alcohols and sugars. These substrates remain the focus of existing research involving improved electron transfer efficiency, enzyme immobilization strategies, and electrode engineering. As the field has advanced in these regards, efforts have also been made to explore more complex enzyme cascades for multistep bioelectrocatalysis of a wider variety of fuels.[1,3,4] An increased degree of enzymatic oxidation of a given fuel provides increased fuel utilization in the instance of a fuel cell and potentially a multiplicative increase in sensitivity for biosensors. When utilizing multiple enzymes in an immobilized electrode configuration, one must consider the interplay between the enzymes and the fate of intermediates involved in a given pathway. Nature has demonstrated a strong propensity for organization of such complex metabolic sequences that optimize efficiency through a given pathway by sequential organization and substrate channeling. It is this added efficiency that this work attempts to mimic by the covalent linkage of sequential enzymes of a two-enzyme process to improve the efficiency of the oxidation of glucose for use in biofuel cell and biosensor applications.

Glucose bioelectrocatalysis has received an enormous level of attention because of its obvious biosensor applications in monitoring the blood glucose levels of diabetic patients and as the main target for implantable biofuel cell and biosensor applications. In addition, if optimized to allow for complete oxidation, glucose provides a readily available high-energy-density fuel. The majority of research in glucose bioelectrocatalysis has focused on improvements made in the utilization of glucose oxidase. Glucose oxidase converts glucose to gluconolactone, requiring O_2 as an electron acceptor to form H_2O_2 as a byproduct. The electron transfer occurs via a flavin adenine dinucleotide cofactor that is attached to the enzyme near the active site, which is submerged deep within the protein structure. The location of the electron acceptor makes the use of this enzyme inefficient because it is incapable of directly channeling electrons to traditional electrode surfaces. Approaches that include low molecular weight diffusive mediators,[5−8] immobilized mediators,[9−14] redox polymer relays,[15−20] and incorporation of nanomaterials[2,21−24] have been made to better access this key electron transfer junction. This enzyme is, however, limited in that it can perform only a one-step, two-electron oxidation of glucose and is oxygen-dependent, if oxygen reduction is not subverted. This results in sensor error associated with frequent changes in blood oxygen content, which is the primary target for this biosensor development.[25]

Received: September 20, 2011
Revised: November 3, 2011
Published: November 08, 2011

Dehydrogenase enzymes provide an alternative to the use of glucose oxidase. Dehydrogenase enzymes such as glucose dehydrogenase differ in that they are not oxygen-dependent and, instead, transfer electrons to other small molecule acceptors (i.e., nicotinimide adenine dinucelotide (NAD^+) in the case of glucose dehydrogenase). Glucose dehydrogenase again oxidizes glucose to gluconolactone, but produces the electron-rich NADH as a byproduct. This eliminates the consideration of oxygen dependence; however, NADH oxidation at common electrode materials requires significant overpotential and has limitations due to significant electrode passivation.[26] A large body of research focuses on improvements in NADH oxidation following approaches similar to that previously mentioned for glucose oxidase.[27,28] Again, nanomaterials offer a simplistic means of addressing these concerns. Carbon nanotubes, in particular, have been demonstrated to lower potentials of NADH oxidation with negligible passivation.[29−31] However, carbon nanotubes are somewhat difficult to incorporate into an enzyme immobilization matrix due to their propensity to aggregate as a result of their high surface energy and attraction toward one another due to hydrophobicity and van der Waals forces.[32]

Glucose dehydrogenase is still limited in that it provides only a single-step oxidation of its target substrate. An ideal biosensor/biofuel cell would take advantage of all extractable energy from glucose, resulting in a more sensitive sensor or a higher-energy-density fuel cell/battery. First demonstrated by Palmore et al. in the complete oxidation of methanol to CO_2 and water, enzymatic cascades provide a platform for accomplishing just that.[33] Recent work has developed means for more complete oxidations of complex fuels through immobilization of several enzymes to immobilizations of complete metabolic pathway components. Substrates such as glycerol, pyruvate, and lactate have been demonstrated to be completely oxidized by increasingly complex cascades immobilized on electrode surfaces, with each additional oxidation step providing benefit to the output of the bioelectrode performance.[1,3,34−36]

One metabolic pathway that accomplishes the multistep oxidation of glucose in biological systems is the oxidative phase of the pentose phosphate pathway. In this pathway, glucose is converted to glucose-6-phosphate (G6P) in the presence of ATP by the action of hexokinase. Following this conversion, G6P is oxidized to 6-phosphogluconolactone by glucose-6-phosphate dehydrogenase (G6PDH). An additional oxidation step occurs following a ring-opening hydrolysis that converts 6-phosphogluconolactone to ribulose-5-phosphate by the action of 6-phosphogluconic dehydrogenase. Each enzyme of this pathway utilizes nicotinimide adenine dinucleotide phosphate ($NADP^+$) as an electron-accepting cofactor that behaves very similarly to NAD^+. If adequately interfaced to an electrode surface, this process would double the output of a single dehydrogenase for each molecule of glucose. However, when utilizing multiple enzymes, mass transfer limitations become increasingly important.

In biological systems, it has been demonstrated that metabolic pathways have evolved to improve mass transfer and kinetic efficiencies of such metabolic pathways. These improvements are achieved through the sequential organization or complexation of the enzymes of a given metabolic pathway. Paul Srere coined the termed *metabolon* to describe such quinary structure and organization of sequential metabolic enzymes.[37,38] Many pathways, including the Krebs cycle, pentose phosphate pathway, and the Calvin cycle, have demonstrated such organization.[39−41] This localization and substrate channeling provides advantages in that it increases local concentrations of a given intermediate for reaction in the next enzymatic process while also lowering the length of diffusion required to reach the next enzyme of the process and protecting potential labile intermediates. This phenomenon can be mimicked toward the advancement of multi-enzyme enzymatic biofuel cells and biosensors through the use of supercomplex formations as bioelectrode catalysts. This will result in an efficient means of a more complete oxidation of a fuel or analyte, providing increased power density or increased signal while optimizing the flux through the metabolic pathway.[25]

Recently, this organization was utilized at a bioanode of a pyruvate/air biofuel cell to demonstrate improved efficiency and power density through controlled sequential organization. This was accomplished through the cross-linking of proteins in intact, purified mitochondria to covalently link sequential enzymes and maintain their natural organization. Once these interactions were made permanent through covalent linkage, the mitochondria were lysed and immobilized to an electrode surface acting as the anodic catalyst in a pyruvate fuel cell. Improvements were shown for samples that were held together with covalent linkage versus samples that were not.[42] However, a great deal of crude material was cast in the immobilization of the mitochondria lysate that was not active for the desired oxidation process. Therefore, it would be advantageous to pursue means for creating a sequentially organized synthetic metabolon that consists only of covalently linked purified enzymes immobilized at an electrode surface.

In this work, researchers take initial steps in examining the improvements in mass transport and efficiency of artificially formed metabolon-based bioelectrocatalysis by examining a two-enzyme, single oxidation of glucose for both sensing and biofuel cell applications and comparing two enzymes that are covalently conjoined and two that are allowed to randomly disperse within an immobilization matrix to quantify improvements in efficiency gained through closer proximity of sequential enzymes. This two-enzyme system is also compared with the performance of a single enzyme system using GDH. Enzymes of interest were immobilized in a previously described dispersed CNT impregnated hydrogel to lower overpotential and passivation of the NAD(P)H cofactor for electrochemical characterization.[43] Improvements were demonstrated for the two-enzyme system relative to the use of the single enzyme GDH. In addition, a covalently linked synthetic metabolon exhibited improved performance as a biosensor and a biofuel cell versus that of randomly dispersed enzyme suspension, demonstrating the potential impact of controlled sequential organization of metabolic proteins. This work proximally localizes two catalytic processes and reduces the length of diffusion of intermediates between two enzyme active sites. Although true substrate channeling between two active sites was not attempted, the covalent localization and sequential organization of the two enzymes resulted in significant improvements in bioanode performance.

EXPERIMENTAL SECTION

Materials. Chemicals such as reduced nicotinimide adenine dinucleotide (NADH), nicotinimide adenine dinucleotide (NAD^+), nicotinimide adenine dinucleotide phosphate ($NADP^+$), adenosine triphosphate (ATP), sodium phosphate, sodium nitrate, glucose, magnesium chloride, L-cysteine, and triethanolamine were purchase from Sigma-Aldrich, St. Louis. Sigma-Aldrich was also the source for enzymes GDH, G6PDH, and hexokinase. Pierce Biotechnolgies

supplied cross-linking reagent 1,11-bismaleimido-triethyleneglycol ($BM(PEG)_3$) and BCA assay reagents. Ethylene glycol diglycidyl ether (EGDGE) was purchased from Polysciences, Inc. Toray paper electrodes were obtained from Fuel Cell Earth, and 3-mm-diameter glassy carbon electrodes were obtained from CH Instruments. Multiwalled carbon nanotubes were purchase from Cheaptubes.com. Octyl-modified linear poly(ethyleneimine) (C8-LPEI) was synthesized as previously described.[43]

Voltammetric/Amperometric Characterization of NADH Oxidation at C8-LPEI/CNT Modified Electrodes. Carbon nanotubes were added to 150 mM solutions of C8-LPEI in various loadings from 0 to 42 mg/mL, which corresponds to 0−66.9 dry wt %. The C8-LPEI/CNT suspensions were sonicated in an ultrasonic bath for ∼30 min. Cyclic voltammetry experiments were carried out on 3-mm-diameter glassy carbon electrodes. To cross-link the polymer/CNT mixtures, C8-LPEI/CNT suspensions were mixed with a 0.3 mol equiv of EGDGE. Prior to curing, 5 μL of the suspension was pipetted directly to the surface of a polished glassy carbon electrode and allowed to dry overnight at room temperature. Electrodes were then tested using a conventional three-electrode setup, and the potential was scanned from 0 to 0.8 V versus a saturated calomel electrode (SCE) using a platinum mesh counter electrode. Experiments were performed in 1 mM NADH in pH 7.0 phosphate buffer containing 100 mM $NaNO_3$ as supporting electrolyte using a CH810 potentiostat (CH Instruments). Each experiment was performed in triplicate using separately constructed electrodes.

Amperometric studies were carried out using the same C8-LPEI/CNT suspension; however, 25 μL of the resultant suspension was cast onto 1 cm^2 Toray paper electrodes, as opposed to 3-mm-diameter glassy carbon electrodes. After curing overnight, electrodes were put in a three-electrode electrochemical cell containing pH 7.0 phosphate buffer and 100 mM sodium nitrate as supporting electrolyte. A potential of 0.4 V was applied to the Toray paper electrode versus SCE and stirred at a constant controlled rate. The potential was chosen as the cyclic voltammetric studies demonstrated peak NADH oxidation with no background interference from the polymer film at this potential. The charging current was allowed to dissipate for >1000 s, and injections of 1 M NADH solution in pH 7.0 phosphate buffer and 100 mM sodium nitrate were made as current as a function of time was monitored. Each experiment was performed in triplicate using separately constructed electrodes.

Amperometric Characterization of GDH and Hexokinase/G6PDH Electrodes. Polymer suspensions were made identically to those previous mentioned; however, prior to casting, 25 Units of enzyme(s) of interest (as determined by product evaluation by Sigma-Aldrich) were introduced to the polymer suspension following the addition of EGDGE, and the mixture was vortexed for ∼30 s to allow for complete mixing. Once mixed, 25 μL of the C8-LPEI/CNT/enzyme suspension was cast onto 1 cm^2 Toray paper and allowed to dry under a fan at room temperature overnight. Glucose dehydrogenase-modified electrodes were then allowed to equilibrate in pH 7.4 phosphate buffer containing 100 mM $NaNO_3$ supporting electrolyte and 1 mM NAD^+. A potential of 0.4 V vs SCE was applied, and charging current was allowed to dissipate for >1000 s. Injections of 2 M glucose solution in the same in pH 7.4 phosphate buffer containing 100 mM $NaNO_3$ supporting electrolyte and 1 mM NAD^+ were made to the convectively stirring solution, and the current was measured as a function of time for varying concentrations of glucose.

Hexokinase/G6PDH electrodes were made in a similar fashion with the C8-LPEI/CNT suspension containing 25 Units of both enzymes prior to casting; however, the buffer solution used was altered because G6PDH is inhibited by phosphate. The buffer for this experiment was 50 mM triethanolamine (pH 7.4) containing 100 mM $NaNO_3$ as supporting electrolyte, 1 mM $NADP^+$, 10 mM $MgCl_2$, and 1 mM ATP. Again, injections of 2 M glucose solution in the same buffer were made to the convectively stirring solution, and current was measured as a function of time for varying concentration of glucose at an applied potential of 0.4 V vs SCE. Each experiment was performed in triplicate using separately constructed electrodes.

Cross-Linking of Hexokinase and G6PDH. This procedure was slightly modified from Pierce Biotechnology suggested usage of $BM(PEG)_3$. A 12.8 mg portion of G6PDH was dissolved in 1 mL of 50 mM triethanolamine (pH 7.0 containing 5 mM EDTA). This results in a 0.1 mM solution of G6PDH, and to this a 2-fold molar excess of $BM(PEG)_3$ was added (10 μL of a 20 mM solution of $BM(PEG)_3$ in DMSO). The solution was allowed to vortex for 1 h at room temperature to attach the cross-linking reagent to solvent-accessible free thiols on the G6PDH structure. This was performed on two samples in parallel, and after 1 h incubation, one of the two samples was exposed to 10-fold molar excess L-cysteine to quench the remaining reactive end of the homobifunctional cross-linker. Excess L-cysteine was removed through buffer exchange centrifugal filtration. This resulted in a non-cross-linked control that maintains simulation of the effects of covalent manipulation of the G6PDH structure. At this point, the remaining test sample and the now quenched control were exposed to a 2-fold molar excess of hexokinase. These two samples were allowed to complete cross-linking of the bienzyme complex (in the case of the test sample) by vortex at room temperature for 1 h.

Enzymatic assays of G6PDH and hexokinase were performed after each step to ascertain unit activity of the product. All enzymatic assays were performed through the spectrophotometric determination of NADPH generation as a function of time in the presence of enzyme substrate through absorbance readings at 340 nm as a function of time. This method was also used to determine final activity of the bienzyme and quenched control product so that equivalent unit activities could be accurately immobilized on electrodes for electrochemical characterization. Protein concentration was quantified by standard BCA procedure.[44] SDS-PAGE was carried out to demonstrate existence of high molecular weight complexes resulting from the test sample and the absence of these high molecular weight complexes in the quenched control sample.

Fuel Cell Bioanode Characterization. Bioanodes were constructed using 25 μL castings of C8-LPEI/CNT/enzyme on 1 cm^2 Toray electrodes as previously mentioned. GDH electrodes were constructed to contain 25 Units of enzyme activity/cm^2. GDH bioanodes were suspended in a 100 mM glucose solution in pH 7.4 phosphate buffer containing 1 mM NAD^+ and 100 mM $NaNO_3$ as supporting electrolyte. This solution was contained in a previously published test cell containing an air breathing cathode, resulting in a glucose/O_2 biofuel cell.[36] This test cell was connected to a CH810 model CH Instruments potentiostat, and the open circuit potential was measured. The open circuit potential was allowed to reach steady state for at least 1000 s, and slow scan (1 mV/s) polarization from the measured open circuit potential to 1 mV was used to generate polarization curves by monitoring current as a function of potential. Hexokinase/G6PDH

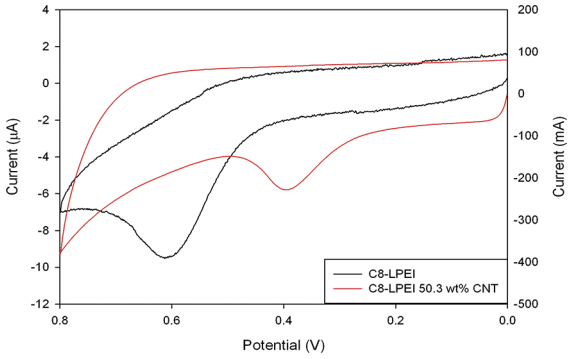

Figure 1. Cyclic voltammograms of NADH using C8-LPEI and C8-LPEI containing 50.3 dry wt % CNT modified electrodes versus SCE (left *Y* axis (C8-LPEI)/right *Y* axis (C8-LPEI with 50.3 wt % CNT).

bienzyme complex and non-cross-linked hexokinase/G6PDH electrodes were tested in the same manner; however, only 5 Units of enzymatic activity were cast per 1 cm^2 electrode due to a limited quantity of the cross-linked product. In addition, an alternative fuel solution consisting of pH 7.4 100 mM glucose, 50 mM triethanolamine, 1 mM $NADP^+$, 1 mM ATP, 10 mM $MgCl_2$, and 100 mM $NaNO_3$ was used. Open circuit potentials and polarization curves were obtained using the same procedure described above for the GDH tested electrodes. Each experiment was performed in triplicate using separately constructed electrodes.

RESULTS AND DISCUSSION

NADH Oxidation at C8-PEI/CNT Modified Electrodes. Initial characterization of this electrode material required exploration of the ability of the dispersed CNT hydrogel composite's ability to facilitate the oxidation of NADH prior to examination of NAD(P)H-dependent enzyme activity at such electrode surfaces. To determine the overpotential reduction achieved through immobilization of dispersed CNTs, cyclic voltammetry was performed on electrodes with CNT loadings from 0 to 66.9 wt % in the presence and absence of 1 mM NADH. Representative data for an electrode coated with C8-LPEI containing no CNTs and an electrode containing 50.3 wt % CNTs in C8-LPEI is demonstrated in Figure 1. The incorporation of CNTs lowered the overpotential for NADH oxidation from 0.585 ± 0.032 V to 0.426 ± 0.019 V. Data used to determine optimal electrode material is demonstrated in Figures S1, S2, and S3 of the Supporting Information. In the absence of NADH, only the electrochemistry associated with the polymer is observed. The incorporation of CNTs to this C8-LPEI film is inherently simple and allows for a potential robustness that often is not seen in typical redox mediators used for NADH oxidation.

This optimal electrode design was also used to examine NADH oxidation at varying scan rates and to examine the transport of NADH through the films. A 50.3 wt % loading was chosen through comparative measurement of peak currents of NADH oxidation as a function of CNT loading. $KD^{1/2}$ values can be determined using the linear relationship between peak current and scan rate,

$$i_p = (2.99 \times 10^5) n\alpha^{1/2} ACKD^{1/2} v^{1/2}$$

where i_p is the peak current for the oxidation wave, n is the number of electrons passed in the reaction, A is the surface area of the electrode, C is the solution bulk concentration of analyte, K is the extraction coefficient, D is the diffusion coefficient of the analyte, and v is the scan rate. Using this relationship, the $KD^{1/2}$ was determined to be 0.039 $cm^2\ s^{-1}$ through the linear relationship of peak current to the square root of scan rate (error was calculated through the standard error of the slope). This value was calculated using the value for the geometric surface area of the glassy carbon electrode; however, the electrochemically accessible surface area of the electrode is significantly higher due to the carbon nanotubes.

In addition, the optimal loading was further reinforced by amperometric measurement of NADH oxidation at 0.4 V vs SCE in a stirred electrochemical cell, from which a sensitivity of 209 ± 7 $\mu A\ mM^{-1}\ cm^{-2}$ was determined from the slope of the linear portion of the calibration curve. Once again, 50.3 wt % loading demonstrated optimal NADH oxidation and reproducibility of electrode construction with amperometric current response leveling significantly for higher CNT loadings. Amperometric data for this optimization is shown in Figures S4 and S5 in the Supporting Information.

Glucose Dehydrogenase Amperometric Biosensor. The LPEI/C8-LPEI hydrogel electrode discussed above was then used to entrap GDH to demonstrate the utilization of this aqueous hydrogel CNT composite's ability to maintain enzyme activity and function as a glucose biosensor. To demonstrate this, an amperometric study of enzyme-catalyzed glucose oxidation at the C8-LPEI/CNT electrode interface was performed utilizing 25 units of enzyme activity per 1 cm^2 electrode. With increasing concentrations of glucose introduced to the convective electrochemical cell, increases in anodic currents were observed. A representative amperometric response for injections of 0−30 mM glucose and an average calibration plot for three electrodes obtained from equivalent procedure are demonstrated in Figure 2A and B. This calibration plot displays a linear range of this sensor electrode from 0.1 to 5 mM with a sensitivity of 10.62 ± 1.22 $\mu A\ mM^{-1}\ cm^{-2}$ glucose.

A kinetics assessment was made through the extrapolation of the amperometric data through Lineweaver−Burk analysis. The Lineweaver−Burk equation relates velocity of reaction to concentration by the following relationship:

$$\frac{1}{v} = \frac{K_m}{V_{max}}\frac{1}{[S]} + \frac{1}{V_{max}}$$

In which v is the reaction velocity, K_m is the Michaelis−Menten constant, V_{max} is the maximum reaction velocity, and $[S]$ is the substrate concentration. The Lineweaver−Burk relationship is displayed in Figure 2C. From this plot, the K_m for the immobilized GDH CNT hydrogel electrode was determined to be 7.48 ± 0.22 mM, and the V_{max} was 41.14 ± 0.08 nM min^{-1}. The error was calculated from the standard error calculation of the slope and intercept of the linear function. The kinetic characterizations of the bioelectrodes tested in this paper are based on solution concentrations of metabolites as an effective equilibrium concentration within the hydrogel film. The true concentration within the modified LPEI film was not determined; however, it was assumed to approximate solution concentrations due to high diffusivity and an assumed lack of strong interaction with the polymer. The bioelectrodes constructed in this work were not tested for their lifetime over an extended period of time. Therefore, the fate of the nicotinamide cofactor and how reliable the recycling of this cofactor is over long periods of time is unknown. In many cases, however, NADH oxidation at CNT-modified electrodes results in a stable amperometric response (not seen with NADH oxidation at planar carbon

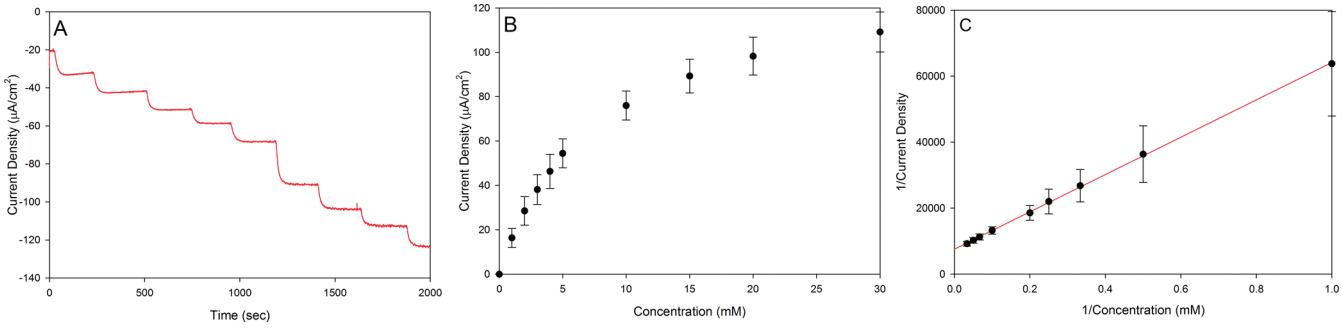

Figure 2. (A) Amperometric response for glucose dehydogenase-modified electrodes in increasing concentrations of glucose (0−30 mM). (B) Calibration curve for glucose dehydrogenase-modified electrodes (error bars = standard deviation). (C) Lineweaver−Burk plot of amperometrically obtained data (error bars = standard deviation).

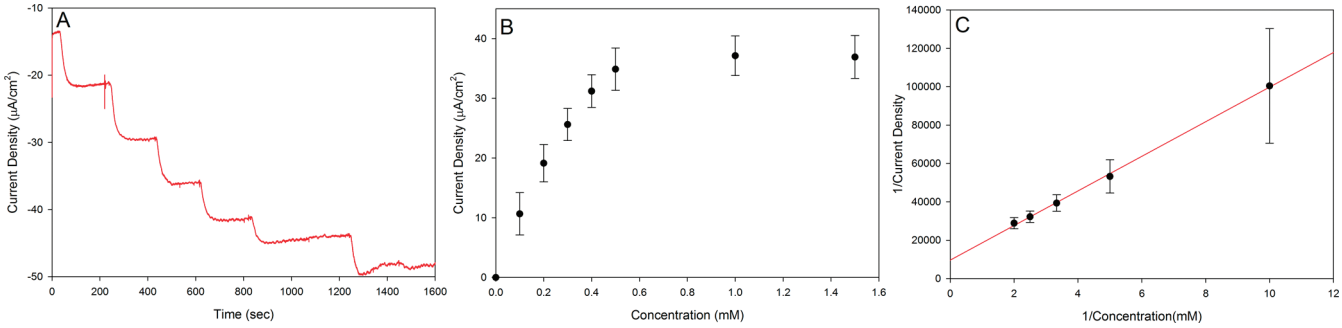

Figure 3. (A) Amperometric response for hexokinase/glucose-6-phosphate dehydrogenase-modified electrodes in increasing concentrations of glucose (0−1.5 mM). (B) Calibration curve for hexokinase/glucose-6-phosphate dehydrogenase-modified electrodes (error bars = standard deviation). (C) Lineweaver−Burk plot of amperometrically obtained data (error bars = standard deviation).

electrodes), indicating the effective recycling of NAD^+ with minimal electrode passivation.[45,46]

Two-Enzyme Amperometric Glucose Biosensor. With the previously mentioned experiments demonstrating that this electrode design was functional as an enzyme immobilization matrix and a glucose biosensor using GDH, hexokinase and G6PDH were immobilized in the same unit activity per square centimeter to accurately compare their characteristics as glucose biosensors. Hexokinase and G6PDH perform a single oxidation of glucose similar to that of GDH but require the phosphorylation of glucose prior to oxidation by the action of hexokinase. Amperometric measurement of the two-enzyme electrode response to glucose gave increased sensitivity in comparison with the GDH-modified electrode. A representative amperometric trace of injections resulting in increasing glucose concentration is shown in Figure 3A, and an average calibration plot is displayed in Figure 3B.

The two-enzyme modified electrodes were examined with lower concentrations of glucose due to an evident reduction in saturation concentration of the two-enzyme system vs the GDH modified electrodes. The linear portion of the calibration plot ranged from 0.1 to 0.5 mM glucose, and the linear portion of the GDH calibration plots ranged from 0.1 to 5 mM. While the linear range of the two-enzyme modified electrode system was reduced, the sensitivity was significantly improved. Again using the linear portion of the calibration plot, a sensitivity of 69.31 ± 7.14 μA mM^{-1} cm^{-2} was calculated. This sensitivity is among the highest reported in the literature for glucose biosensors and shows the promise of the hexokinase/G6PDH system in this area.[47−51]

The Lineweaver−Burk relationship is displayed for the two-enzyme modified electrodes in Figure 3C. Again, this linear relationship was used to determine the K_m (0.93 ± 0.20 mM) and V_{max} (32.27 ± 0.37 nM/min). The error was calculated from the standard error calculation of the slope and intercept of the linear function. The key characteristics of the GDH and hexokinase/G6PDH electrodes are directly compared in Table 1. The reduced saturation level of this two-enzyme biosensor electrode is demonstrated in the reduced V_{max}. The very low K_m for the two-enzyme system demonstrates the very high affinity glucose has for this two-enzyme system, resulting in higher sensitivity due to the system's approaching maximum reaction velocity at a quicker rate. Most significantly, there was a >5.5-fold increase in sensitivity for the two-enzyme electrode vs the GDH electrode that results from these improved enzyme kinetics. We recognize that this kinetic approximation of the hydrogel bioelectrode performance is not physically meaningful for the true enzyme kinetics due to the fact that this is a multi-enzyme system immobilized in a hydrogel. However, this approximation grants the ability to relatively compare electrode performance by examining the electrode simply as a combined catalyst. Due to this fact, comparison to literature values for kinetic values of individual enzymes in solution would be inappropriate. However, in comparison with recent efforts for similar immobilized glucose oxidizing electrodes, values obtained in this study compare favorably. The K_m value calculated for this biosensor is lower than most found in contemporary literature, demonstrating the electrode's high affinity for glucose, and the measured sensitivity is significantly higher than contemporary glucose biosensor work that was tabulated by Pradhan et al.[52]

dx.doi.org/10.1021/cs200482v |*ACS Catal.* 2012, 2, 17–25

Cross-Linking of Hexokinase and G6PDH. Hexokinase and G6PDH are advantageous in this study not only because of their significant activity in the immobilization matrix chosen for this work, but also because of their amino acid composition. In examining means for bioconjugation of two enzymes, one must look at the availability/abundance of functional groups within the target proteins' amino acid primary structure. In attempting to maintain optimal enzyme activity, one must take care to not overly manipulate the native protein structure while utilizing solvent-accessible functional groups on both proteins to promote linkage. In this case, the two enzymes contain minimal cysteine (Cys) residues in their primary structure (one Cys in GDH and four Cys in hexokinase). The single solvent Cys residue in G6PDH allows for directed linkage of G6PDH to hexokinase through a simple sequence of reaction with a thiol reactive homobifunctional cross-linker.

A schematic for the chosen reaction scheme is demonstrated in Figure 4. $BM(PEG)_3$ first reacts with the single free thiol of G6PDH, not only activating the protein for cross-linking to another free thiol but also protecting the only free thiol in the structure of G6PDH. Therefore, when the activated G6PDH is exposed to hexokinase, the only accessible reaction sites are contained in hexokinase, causing preferential G6PDH to hexokinase as opposed to self-cross-linking of the G6PDH. Figure 5 shows an example SDS PAGE for a sample that is cross-linked as previously described and a sample that is quenched prior to exposure to hexokinase. This demonstrates the formation of high-molecular-weight complexation for the cross-linked sample and a lack of G6PDH-G6PDH cross-linking that would be present in the quenched sample but is not visible. SDS PAGE demonstrates a successful and specific cross-linking of G6PDH to hexokinase that can be used to demonstrate the potential advantages of sequential organization in the construction of a multi-enzyme bioanode of a glucose biofuel cell.

Table 1. Comparison of Data Obtained from Lineweaver-Burk Analysis and Calibration Plots of Glucose Dehydrogenase-Modified Electrode versus Hexokinase/Glucose-6-phosphate Dehydrogenase-Modified Electrodes

	K_m (mM)	V_{max} (nM/min)	sensitivity (μA/mM cm^2)
glucose dehydrogenase	7.48 ± 0.22	41.14 ± 0.08	10.62 ± 1.22
hexokinase and glucose-6-phosphate dehydrogenase	0.93 ± 0.20	32.27 ± 0.37	69.31 ± 7.14

Cross-Linked Enzymatic Bioanode vs Noncross-Linked Bioanodes Performance in a Glucose/Air Biofuel Cell. As research concerning enzymatic bioelectrodes has increased in efforts toward the use of multi-enzyme oxidation of a given substrate to combat limited oxidation of enzymatic bioelectrodes, one must begin to optimize the interaction of the multi-enzyme systems and explore increases in efficiency associated with improved mass transport of an intermediate substrate between two enzymes. The following study attempts to address

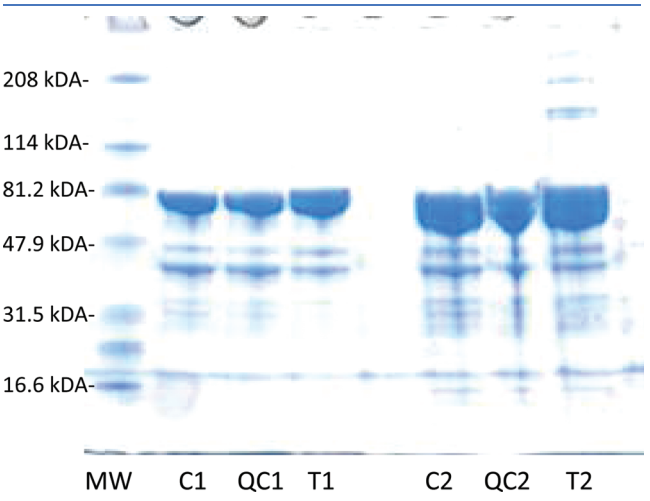

Figure 5. SDS−PAGE of homobifunctional cross-linking of G6PDH and hexokinase. C = control sample containing no cross-linking reagent. QC = sample in which cross-linker was quenched prior to bienzyme complex formation. T = active cross-linker sample. Samples 1 taken prior to enzyme combination; samples 2 taken after enzyme combination. MW = molecular weight marker.

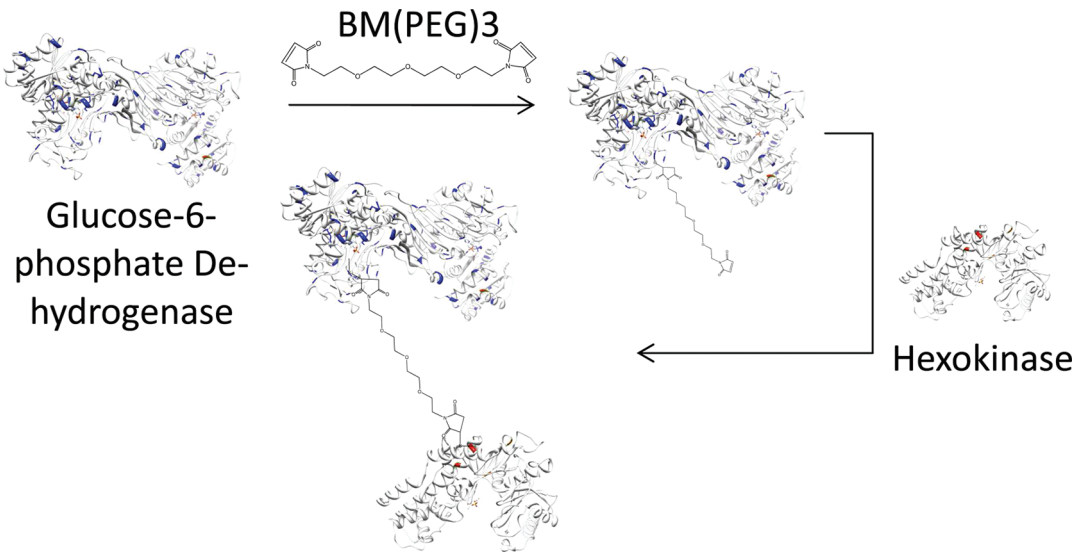

Figure 4. Schematic representation of homobifunctional cross-linking of hexokinase to glucose-6-phosphate dehydrogenase using $BM(PEG)_3$.

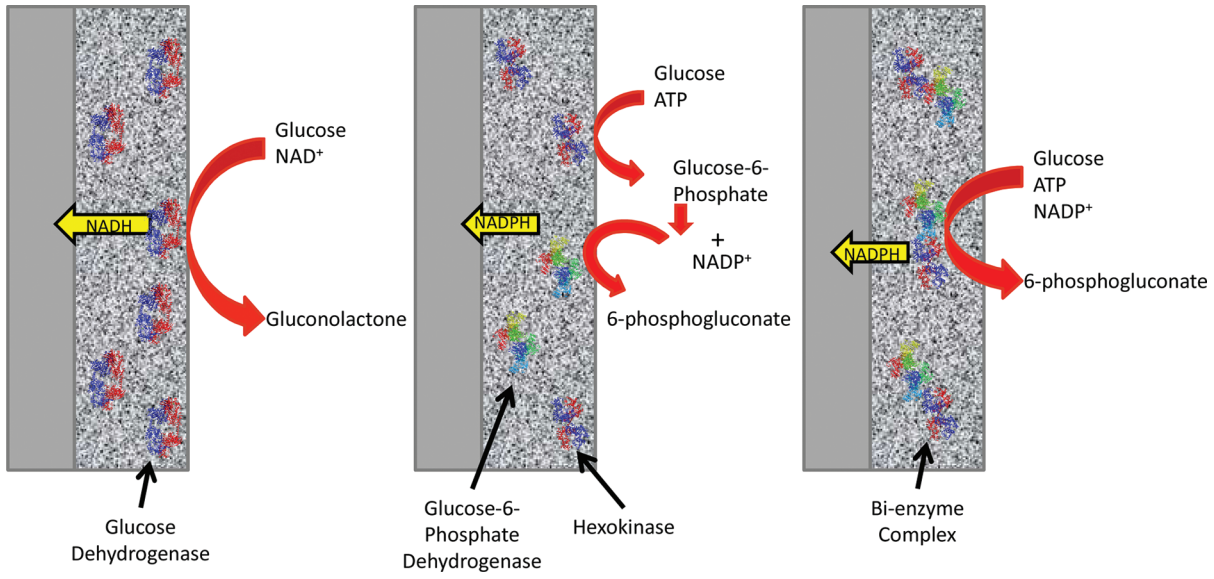

Figure 6. Schematic representation of the three types of fuel cell electrodes tested: (left) glucose dehydrogenase-modified, (middle) hexokinase and glucose-6-phosphate dehydrogenase immobilized randomly, and (right) cross-linked bienzyme complex modified electrodes.

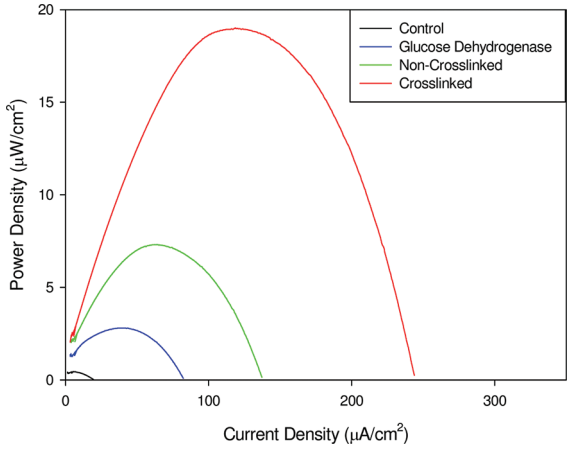

Figure 7. Representative power curves obtained from (1) a control electrode (containing no enzyme), (2) a glucose dehydrogenase-modified electrode, (3) a non-cross-linked hexokinase/glucose-6-phosphate dehydrogenase-modified electrode, and (4) a cross-linked hexokinase/glucose-6-phosphate dehydrogenase-modified electrode.

this potential increase in efficiency through the covalent linkage of sequential enzymes while exploring projected improvements in performance as a bioanode in a biofuel cell. This effort attempts to mimic the formation of a metabolon to enhance the performance of a two-enzyme modified electrode.

This concept is depicted in Figure 6. Bioanodes were constructed by previously mentioned means to contain 25 Units cm^{-2} GDH, 5 Units cm^{-2} of both hexokinase and G6PDH randomly dispersed, or 5 Units cm^{-2} of both hexokinase and G6PDH that had been previously covalently linked, as previously mentioned. This covalent linkage should result in reduced diffusional lengths for the intraenzyme intermediate to travel, thereby eliminating diffusion through the polymer matrix between enzymes. This improvement in mass transport efficiency was examined through improvements in bioanode performance.

Table 2. Comparison of Data Obtained Glucose/Air Biofuel Cell Anodes for Control Containing No Enzyme, Glucose Dehydrogenase-Modified Electrode, Non-cross-linked Hexokinase/Glucose-6-phosphate Dehydrogenase-Modified Electrode, and Cross-linked Hexokinase/Glucose-6-phosphate Dehydrogenase-Modified Electrode

	open circuit potential (V)	maximum current density ($\mu A/cm^2$)	maximum power density ($\mu W/cm^2$)
control	0.291 ± 0.016	23.01 ± 3.27	0.531 ± 0.102
glucose dehydrogenase	0.410 ± 0.003	69.58 ± 24.49	3.22 ± 1.23
two enzyme non-cross-linked	0.507 ± 0.005	132.0 ± 5.6	6.73 ± 0.60
bienzyme complex	0.604 ± 0.025	235.0 ± 35.8	20.60 ± 7.68

GDH-modified electrodes were tested in a glucose/air biofuel cell to allow for comparison with the two-enzyme systems. The GDH C8-LPEI/CNT bioanode resulted in an open circuit potential of 0.410 ± 0.003 V vs the platinum catalyzed air-breathing cathode. The maximum current density of this fuel cell was 69.58 ± 24.49 $\mu A\ cm^{-2}$, and the maximum power density was 0.531 ± 0.102 $\mu W\ cm^{-2}$. This maximum current density was significantly lower than what was achieved in the amperometric study of identical electrodes, likely due to the quiescent conditions of the fuel cell that reduced convection of NAD and glucose to the electrode surface due to the lack of stirring.

The non-cross-linked hexokinase/G6PDH C8-LPEI/CNT electrodes outperformed the GDH electrodes using less unit activity per unit area. This two-enzyme system nearly doubled the performance of the GDH bioanode, resulting in an average maximum current density of 132.0 ± 5.6 $\mu A\ cm^{-2}$ and an average maximum power density of 6.73 ± 0.60 $\mu W\ cm^{-2}$. This increase in performance compared with the GDH-modified electrode is speculated to result from the increased affinity of glucose to the immobilized enzymes, as demonstrated by the previously mentioned Lineweaver−Burk analysis and also potential

dx.doi.org/10.1021/cs200482v |ACS Catal. 2012, 2, 17–25

increased stability of these particular enzymes in the surfactant-like immobilization matrix in comparison with GDH.

In support of the hypothesis that covalent linkage of the two enzymes would result in improvements in mass transport efficiencies and, thus, improved bioanode performance, the cross-linked hexokinase/G6PDH C8-LPEI/CNT bioanodes demonstrated a ~78% increase in maximum current density and over double the maximum power density of the non-cross-linked bioanodes. The average maximum current density was 235.0 ± 35.8 μA cm^{-2}, and the average maximum power density was 20.60 ± 7.68 μW cm^{-2} for three individually constructed bioanodes. Representative power curves for all three electrode manifestations are displayed in Figure 7 as compared with a control electrode containing no enzyme.

Key analytical characteristics of the given bioanodes in biofuel cells are also directly compared in Table 2. These results demonstrate the importance of interenzyme substrate mass transport efficiency. In utilizing polymer immobilization matrixes, this effect is heightened because of the slow diffusion in the polymer matrix between enzymes. This effect is speculated to be compounded in the case of a more complex multi-enzyme oxidation containing more than two enzymes. We also recognize that recent literature has demonstrated that in amphiphilic polymer matrixes, proteins can have an increased propensity for aggregation,[53] which could play a role in the results described above. Protein aggregation in the specific polymer used in this study has not been investigated to date, but will be a focus of future studies.

CONCLUSION

As researchers begin to address the issue of incomplete oxidation of simplistic enzymatic biofuel cells with more complex multi-enzyme systems, the interenzyme localization of substrate over short distances becomes of supreme importance, as demonstrated by these results for this two-enzyme, single oxidation system. This abbreviated pentose phosphate pathway mimic not only demonstrated advantages of sequential organization of the bioanode of an enzymatic biofuel cell; but also demonstrated performance improvements as a biosensor and biofuel cell electrode when compared with the single enzyme electrode utilizing GDH as the catalyst. Further improvements that use the cross-linking methodology outlined in this manuscript for incorporation of a third enzyme (6-phosphogluconic dehydrogenase) to complete the oxidative phase of the pentose phosphate pathway and explore alternative means for constructing substrate channeled bioelectrodes will be explored.

ASSOCIATED CONTENT

Supporting Information. Procedures and results demonstrating optimization of CNT loading in C8-LPEI for the oxidation of NADH are described in the Supporting Information. This information is available free of charge via the Internet at http://pubs.acs.org/.

AUTHOR INFORMATION

Corresponding Author

*Phone: 801-587-8325. Fax: 801-581-8181. E-mail: minteer@chem.utah.edu.

ACKNOWLEDGMENT

The authors thank the Air Force Research Laboratory, National Science Foundation, and Leonard Wood Institute for funding.

REFERENCES

(1) Sokic-Lazic, D.; Minteer, S. D. *Electrochem. Solid State Lett.* **2009**, *12*, F26.
(2) Zebda, A.; Chantal, G.; Le Goff, A.; Holzinger, M.; Cinquin, P.; Cosnier, S. *Nature Comm.* **2011**, *2*, 1.
(3) Arechederra, R. L.; Minteer, S. D. *Fuel Cells* **2009**, *9*, 63.
(4) Treu, B. L.; Minteer, D. S. *Bioelectrochemistry* **2008**, *74*, 73.
(5) Cass, A. E. G.; Davis, G.; Francis, G. D.; Hill, H. A. O.; Aston, W. J.; Higgins, I. J.; Plotkin, E. V.; Scott, L. D. L.; Turner, A. P. F. *Anal. Chem.* **1984**, *56*, 667.
(6) Battaglini, F.; Calvo, E. J. *J. Chem. Soc. Faraday Trans.* **1994**, *90*, 987.
(7) Vaillancourt, M.; Chen, J. W.; Fortier, G.; Belanger, D. *Electroanalysis* **1998**, *11*, 23.
(8) Gao, Z.; Xie, F.; Shariff, M.; Arshas, M.; Ying, J. Y. *Sens. Actuators, B* **2005**, *111−112*, 339.
(9) Yu, C.; Yen, M.; Chen, L. *Biosens. Bioelectron.* **2010**, *25*, 2515.
(10) Degani, Y.; Heller, A. *J. Am. Chem. Soc.* **1989**, *111*, 2357.
(11) Forrow, N. J.; Walters, S. J. *Biosens. Bioelectron.* **2004**, *19*, 763.
(12) Hu, J.; Turner, A. P. F. *Anal. Lett.* **1991**, *24*, 15.
(13) Kulys, J.; Hansen, H. E.; Buch-Rasmussen, T.; Wang, J.; Ozsoz, M. *Anal. Chim. Acta* **1994**, *288*, 193.
(14) Sung, W. J.; Bae, Y. H. *Anal. Chem.* **2000**, *72*, 2177.
(15) Calvo, E. J. *J. Electroanal. Chem.* **1994**, *369*, 279.
(16) Koopal, C. G. J.; de Ruiter, B.; Nolte, R. J. M. *J. Chem. Soc., Chem. Commun* **1991**, *23*, 1691.
(17) Calvo, E. J.; Etchenique, R.; Pietrasanta, L.; Wolosiuk, A. *Anal. Chem.* **2001**, 73.
(18) Calabrese Barton, S.; Sun, Y.; Chandra, B.; White, S.; Hone, J. *Electrochem. Solid State Lett.* **2007**, *10*, B96.
(19) Flexer, V.; Calvo, E. J.; Bartlett, P. N. *J. Electroanal. Chem.* **2010**, 646.
(20) Meredith, M. T.; Kao, D.; Hickey, D.; Schmidtke, D. W.; Glatzhofer, D. T. *J. Electrochem. Soc.* **2011**, *158*, B166.
(21) Wang, J.; Musameh, M. *Anal. Chim. Acta* **2005**, *539*, 209.
(22) Wang, S. C.; Yang, F.; Silva, M.; Zarow, A.; Wang, Y.; Iqbal, Z. *Electrochem. Commun.* **2009**, *11*, 34.
(23) Wang, J. *Chem. Rev.* **2008**, *108*, 814.
(24) Bullen, R. A.; Arnot, T. C.; Lakeman, J. B.; Walsh, F. C. *Biosens. Bioelectron.* **2006**, *21*, 2015.
(25) Moehlenbrock, M. J.; Toby, T. K.; Pelster, L. N.; Minteer, S. D. *ChemCatChem* **2011**, *3*, 561.
(26) Moehlenbrock, M. J.; Minteer, S. D. *Chem. Soc. Rev.* **2008**, *37*, 1188.
(27) Karyakin, A. A.; Karyakina, E. E.; Schuhmann, W.; Schmidt, H. L. *Electroanalysis* **1999**, *11*, 553.
(28) Wang, Y.; You, C.; Zhang, S.; Kong, J.; Marty, J. L.; Zhao, D.; Liu, B. *Microchim. Acta* **2009**, *167*, 75.
(29) Wooten, M.; Gorski, W. *Anal. Chem.* **2010**, *82*, 1299.
(30) Musameh, M.; Wang, J.; Merkoci, A.; Lin, Y. *Electrochem. Commun.* **2002**, *4*, 743.
(31) Zhang, M.; Gorski, W. *Anal. Chem.* **2005**, *77*, 3960.
(32) Hu, L.; Hecht, D. S.; Gruner, G. *Chem. Rev.* **2010**, *110*, 5790.
(33) Palmore, G.; Bertschy, H.; Bergens, S. H.; Whitesides, G. M. *J. Electroanal. Chem.* **1998**, *443*, 155.
(34) Sokic-Lazic, D.; Arechederra, R. L.; Treu, B. L.; Minteer, S. D. *Electroanalysis* **2010**, *22*, 757–764.
(35) Sokic-Lazic, D.; Minteer, S. D. *Biosens. Bioelectron.* **2008**, *24*, 945.
(36) Arechederra, R. L.; Treu, B. L.; Minteer, S. D. *J. Power Sources* **2007**, *173*, 156.
(37) D'Souza, S. F.; Srere, P. A. *Biochim. Biophys. Acta* **1983**, *724*, 40.
(38) Srere, P. A. *Trends Biochem. Sci.* **1985**, *10*, 109.
(39) Velot, C.; Mixon, M. B.; Teige, M.; Srere, P. A. *Biochemistry* **1997**, *36*, 14271.
(40) Debnam, P. M.; Shearer, G.; Blackwood, L.; Kohl, D. H. *Eur. J. Biochem.* **1997**, *246*, 283.

(41) Winkel, B. S. J. *Annu. Rev. Plant Biol.* **2004**, *55*, 85.
(42) Moehlenbrock, M. J.; Toby, T. K.; Waheed, A.; Minteer, S. D. *J. Am. Chem. Soc.* **2010**, *132*, 6288.
(43) Moehlenbrock, M. J.; Meredith, M. T.; Minteer, S. D. *MRS Commun*. DOI: 10.1557/mrc.2011.12. Published Online: **2011**.
(44) Smith, P. K.; Krohn, R. I.; Hermanson, G. T.; Mallia, A. K.; Gartner, F. H.; Provenzano, M. D.; Fujimoto, E. K.; Goeke, N. M.; Olson, B. J.; Klenk, D. C. *Anal. Biochem.* **1985**, *150*, 76.
(45) Musameh, M.; Wang, J.; Merkoci, A.; Lin, Y. *Electrochem. Commun.* **2002**, *4*, 743.
(46) Wang, J.; Musameh, M. *Anal. Lett.* **2003**, *36*, 2041.
(47) Si, P.; Kannana, P.; Guoa, L.; Sonb, H.; Kima, D. *Biosens. Bioelectron.* **2011**, *26*, 3845.
(48) Bunte, C.; Prucker, O.; Konig, T.; Ruhe, J. *Langmuir* **2009**, *8*, 6019.
(49) Merchant, S. A.; Meredith, M. T.; Tran, T. O.; Brunski, D. B.; Johnson, M. B.; Glatzhofer, D. T.; Schmidtke, D. W. *J. Phys. Chem. C* **2010**, *114*, 11627.
(50) Deng, L.; Liu, Y.; Yang, G.; Shang, L.; Wen, D.; Wang, F.; Xu, Z.; Dong, S. *Biomacromolecules* **2007**, *8*, 2063.
(51) Qiu, J.; Zhou, W.; Guo, J.; Wang, R.; Liang, R. *Anal. Biochem.* **2009**, *385*, 264.
(52) Pradhan, D.; Niroui, F.; Leung, K. T. *Appl. Mater. Interfaces* **2010**, *2*, 2409.
(53) Martin, G. L.; Minteer, S. D.; Cooney, M. *Chem. Comm* **2011**, *47*, 2083.